Applied Catalysis A: General 464–465 (2013) 35–42

Contents lists available at SciVerse ScienceDirect

Applied Catalysis A: General

journal homepage: www.elsevier.com/locate/apcata

Polymerization of 1,3-butadiene catalyzed by pincer cobalt(II) complexes derived from 2-(1-arylimino)-6-(pyrazol-1-yl)pyridine ligands

Dirong Gong[a,b], Weiguo Jia[a], Tao Chen[a], Kuo-Wei Huang[a,*]

[a] King Abdullah University of Science and Technology (KAUST), Division of Physical Sciences and Engineering and KAUST Catalysis Center, Thuwal 23955-6900, Saudi Arabia
[b] Department of Polymer Science and Engineering, Ningbo University, Ningbo, 315211, China

ARTICLE INFO

Article history:
Received 23 November 2012
Received in revised form 24 February 2013
Accepted 17 April 2013
Available online xxx

Keywords:
Cobalt(II) complexes
2-(1-Arylimino)-6-(pyrazol-1-yl)pyridine
1,3-Butadiene
Selectivity
Polybutadiene

ABSTRACT

A new class of air stable and structurally well-defined cobalt complexes with unsymmetrical pincer type ligands ([2-(ArN=CMe)-6-(Py)C_5H_3N]$CoCl_2$) (Ar = —C_6H_5, Py = pyrazol-1-yl, **5a**; Ar = 2,4,6-$Me_3C_6H_2$, Py = pyrazol-1-yl, **5b**; Ar = 2,6-$^iPr_2C_6H_3$, Py = pyrazol-1-yl, **5c**; Ar = —C_6H_5, Py = 3,5-Me_2pyrazol-1-yl, **5d**; Ar = 2,4,6-$Me_3C_6H_2$, Py = 3,5-Me_2pyrazol-1-yl, **5e**; Ar = 2,6-$^iPr_2C_6H_3$, Py = 3,5-Me_2pyrazol-1-yl, **5f**; Ar = 2,6-$^iPr_2C_6H_3$, Py = 3,5-$^iPr_2$pyrazol-1-yl, **5g** and [2-(O=CMe)-6-(3,5-diphenylpyrazol-1-yl)C_5H_3N]$CoCl_2$ **5h**) were prepared and the molecular structures of **5a**, **5c** and **5f** were determined by single crystal X-ray crystallography. Upon activation by methylaluminoxane (MAO) in toluene at room temperature, all complexes initiate polymerization of 1,3-butadiene (polymer yields: 65–99%), affording polybutadiene with excellent *cis*-1,4 regularity (97.5–98.7%). The polymer yields and properties in terms of molecular weight and distribution are well controlled by the substituents on iminoaryl rings and pyrazole rings. Selectivity switch from *cis*-1,4 to syndio-1,2 was also achievable by adding phosphine as microstructure regulator.

1. Introduction

Polymerization of 1,3-butadiene is an important process in the polymer industry as the resultant polymers possess versatile properties for a wide range of applications [1–3]. As these properties depend mainly on the microstructures generated during the polymerization, much effort has been devoted to designing highly regio- and/or stereoselective catalyst systems, to prepare polybutadienes with precisely tailor-made microstructures. The development of homogeneous Ziegler–Natta catalysts has realized regio- and stereospecific polymerization of 1,3-butadiene to produce *cis*-1,4- [4–11], *trans*-1,4- [9,12–16] and syndiotactic 1,2-polybutadienes [17–31]. Among them, *cis*-1,4-polybutadiene is one of the most important products since it is employed as one of the major materials in the tire and automotive industries [32]. *Cis*-1,4-polybutadiene can also be copolymerized or blended with other compounds to prepare materials with improved mechanical properties, such as Styrene-Butadiene Rubber (SBR), High Impact PolyStyrene (HIPS), Acrylonitrile-Butadiene-Styrene (ABS) or Hydroxyl Terminated PolyButadiene (HTPB). As a result, transition metal complexes have been considerably explored as catalyst precursors to prepare the *cis*-1,4 polymer [33]. Ziegler–Natta catalysts of titanium [34–38], nickel [39–41], cobalt [17,33,42–51] and neodymium-based catalysts [2,8,11,52–55] activated with various organoaluminum reagents have been used in the production of *cis*-1,4-polybutadiene, with the neodymium-based ones being the main catalysts used for the production on the industrial scale. These catalysts offer high activity and selectivity (*cis*-1,4 > 97%) to provide polymers with desirable material properties such as excellent abrasion and cracking resistance and high tensile strength of the vulcanizates [6]. Their ill-defined and multi-site nature, nevertheless, causes relatively broad molecular weight distributions, and thus complicates the mechanistic study and hinder catalyst design and optimization. In order to gain better control over molecular weight and polymer compositions, academic and industrial research has focused on well-defined single-site catalysts in recent years, mainly based on rare earth metals and the first row transition metals. Various well-defined Ln—C bond containing complexes, such as lanthanide-based metallocene alkyl complexes, lanthanocene aluminates, alkyl bridged lanthanide carboxylates, and lanthanide alkyl complexes supported by versatile pincer ligands, are extensively investigated and developed [1,2,5,56–59]. With these active systems, excellent controls over the molecular weights as well as the microstructures of polymers are facilely achieved, though industrial applications have not yet been demonstrated. Meanwhile, late transition metal catalysts, such as iron,

* Corresponding author. Tel.: +966 2 8080328; fax: +966 2 8081025.
E-mail address: hkw@kaust.edu.sa (K.-W. Huang).

0926-860X/$ – see front matter © 2013 Elsevier B.V. All rights reserved.
http://dx.doi.org/10.1016/j.apcata.2013.04.026

nickel and cobalt, have been received increased attention due to their good functional group tolerance, decreased air and moisture sensitivity and lower cost and environmental impact. In particular, cobalt-based catalysts have been demonstrated for high regio- and stereoselective polymerization of 1,3-butadiene [60].

The carboxylates (or acetylacetonate) [61,62] and halides of cobalt [17,31,33,42–45,47,49] are the major classes of catalysts for producing *cis*-1,4-polybutadiene when activated by methylaluminoxane (MAO) or aluminum chlorides. Simple cobalt salts $CoCl_2$, activated with organoaluminum compounds, are able to generate heterogeneous active species to polymerize 1,3-butadiene with *cis*-specific living polymerization. Interestingly, in the polymerization process, the selectivity can be switched and led to the formation of desired *cis*-1,4-1,2 block copolymer by addition of PPh_3 [17,47,49]. Homogeneous systems such as $Co(acac)_3$ [61] and $Co(Salen)_2$ [42,63] in combination with MAO or ethyl aluminum sesquichloride (EAS) were also reported to catalyze *cis*-regiospecific polymerization of 1,3-butadiene. More recently, research efforts in this field have been gradually shifted on the design of well-defined, homogeneous and high active $CoCl_2$ complexes supported with various tridentate ligands, such as bis(imino)pyridine, bis(imidazolyl)amine and bis(imidazolyl)pyridine, and the high *cis*-1,4 selectivity and activity have been maintained [9,16,33,44,64–68]. Despite these achievements, further exploration of well-defined homogeneous catalyst systems with high *cis*-1,4 selectivity and thermo-, air and moisture stability has remained a fascinating and challenging subject. We are interested in pincer ligated complexes in a general formula of [(NNL)M] because their coordination geometries and electronic properties (and thus the reactivity of the metal center) could be modified by tuning the structures of the arms and substituents [60]. When the pyridyl-supported pyrazolyl-imine system is adopted, the large π-system is believed to increase the Lewis-acidity of the metal center to facilitate the interactions between the metal and the monomer which may enhance the activity [69]. Herein, we describe the synthesis and characterization of a new class of cobalt complexes with pyridyl-supported pyrazolyl-imine ligands and their applications in the 1,3-butadiene polymerization.

2. Results and discussion

2.1. Synthesis and characterization of complexes

The cobalt complexes **5a–5g** were obtained by reacting $CoCl_2$ with one equivalent of corresponding ligands at room temperature (Scheme 1). These complexes were characterized by IR, and elemental analysis, as well as single crystal X-ray analysis of the selected compounds. The C=N (arylimino) stretching bands of free ligands at 1649–1631 cm^{-1} shift toward lower frequencies by 7–23 cm^{-1} when coordinated to cobalt. The structures of **5a**, **5c** and **5f** were further confirmed by X-ray crystallography.

The molecular structure of **5a** shows it is an ion-paired complex $[L_2Co]^{2+}[CoCl_4]^{2-}$ (Fig. 1). The cobalt center in the cation of **5a** is six-coordinate, with Co—N (imino nitrogen and pyrazole nitrogen) bonds ranging from 2.004 to 2.140 Å. These bonds are shorter by 0.04–0.07 Å than those observed in complexes **5c** and **5f**. The geometry of **5c** shows a distorted trigonal bipyramidal structure with the N1—Cl1—Cl2 equatorial plane (Fig. 2). The cobalt atom slightly lies 0.0078 Å out of the plane with three equatorial angles of 92.0° (N1—Co1—Cl2), 115.9° (Cl2—Co1—Cl1) and 151.8° (N1—Co1—Cl1). The equatorial plane is almost perpendicular to both of the pyrazole and pyridine planes, with dihedral angles of 88.7° and 89.6°, respectively. The dihedral angle between the pyridine and the iminoary plane is 88.9°. The Co1—N1 (pyridine) bond is 0.087 Å shorter than the Co1—N3 (pyrazole) bond (2.164 Å) and 0.113 Å shorter than

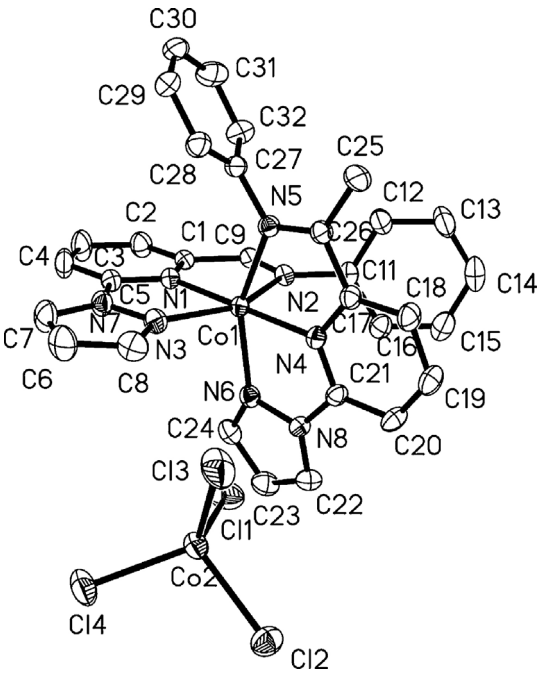

Fig. 1. ORTEP drawing of cationic complex **5a** with thermal ellipsoids at the 30% probability level. Hydrogen atoms have been omitted for clarity.

the Co1—N2 (iminoaryl) bond (2.190 Å), respectively. The Co1—Cl2 bond is 0.078 Å longer than the Co1—Cl1 bond (2.310 vs. 2.232 Å). The imino N(2)—C(6) bond length is 1.284 Å, with the typical character of a C=N double bond.

The unit cell of complex **5f** contains two independent molecules (Fig. 3), with only few differences in the coordination geometry of the central metals. Interestingly, the distance between two planes of pyrazole rings is approx. 3.4 Å, suggesting certain degree of π-π stacking stabilization in the solid state. The geometrical parameters are comparable to those in **5c**, but the N2—Co1—N3 and N6—Co1—N7 angles of **5f** are slightly larger than the N2—Co1—N3 angle in **5c** (144.0 and 142.2 vs. 139.2, respectively). The imino N—C bond lengths of 1.285 and 1.282 Å indicate the C=N double bond character.

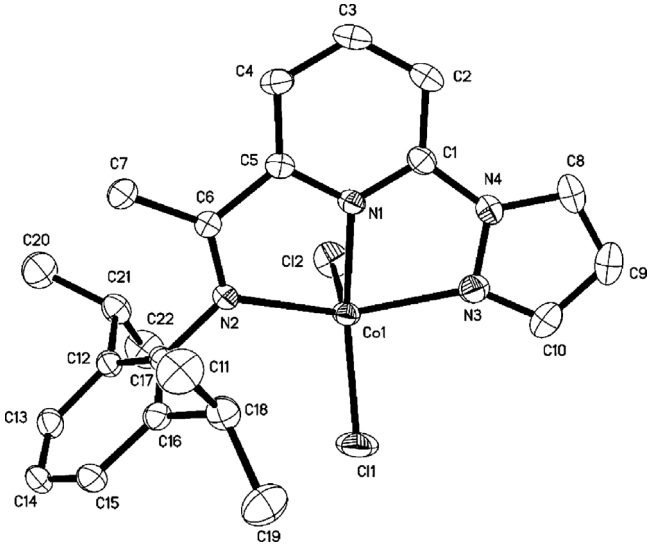

Fig. 2. ORTEP drawing of **5c** with thermal ellipsoids at the 30% probability level. Hydrogen atoms have been omitted for clarity.

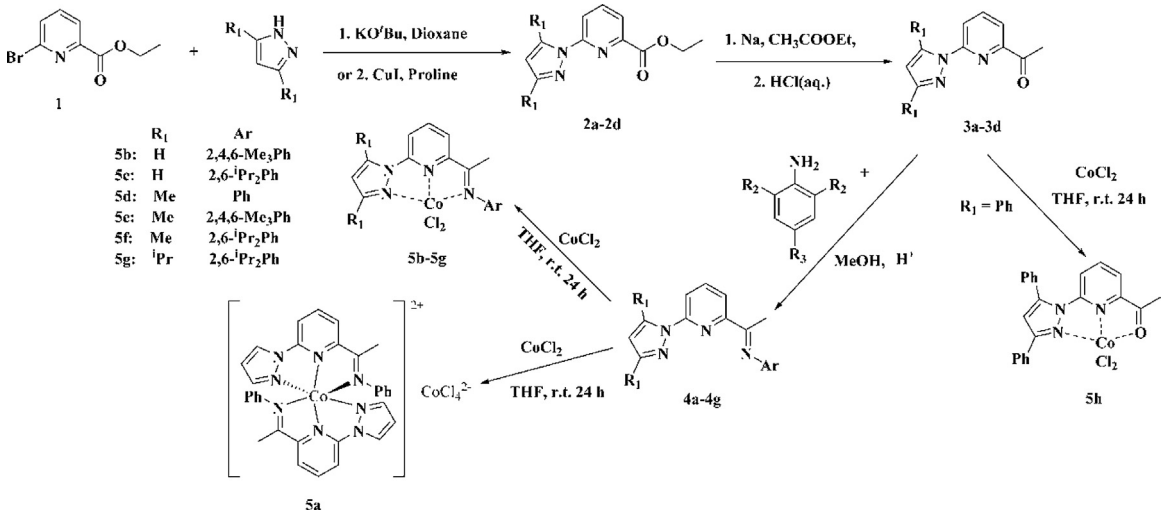

Scheme 1. Synthesis of ligands and the corresponding cobalt complexes.

2.2. Butadiene polymerization behaviors of complexes activated by MAO

2.2.1. Polymerization conditions optimization

The influences of the MAO/Co molar ratio and the reaction temperatures on the 1,3-butadiene polymerizations were investigated in detail with complex **5c** as the catalyst precursor (Table 1). An obvious increase in the production of polymer was observed when elevating the polymerization temperatures from 0 to 40 °C (entries 1–3). However, a further increase from 40 °C to 80 °C resulted in decreased productivities, presumably due to the deactivation of the active centers (entries 4 and 5) [45]. At the same time, the higher polymerization temperature also led to a higher PDI (entries 1–5), suggesting an increase in the β-hydrogen elimination rate relative to the propagation rate at a higher temperature. Analysis on the microstructures of the resulting polymers revealed that increasing the temperature led to a slight decrease in the *cis*-1,4 selectivity, consistent with the literature observations [2]. For example, the selectivity for *cis*-1,4 decreased from 98.7% at 0 °C to 97.2% at 80 °C. A higher MAO/Co molar ratio generally led to a higher monomer conversion. When the ratio of MAO/Co was 600, the catalytic system reached the highest monomer conversion of up to 83%. The selectivity of the resulting polymer structure, however, was not strongly affected by the MAO/Co ratio (entries 2, 6–9). The PDI of polymer decreased first, and then increased with increasing of the MAO/Co molar ratio (entries 2, 6–9).

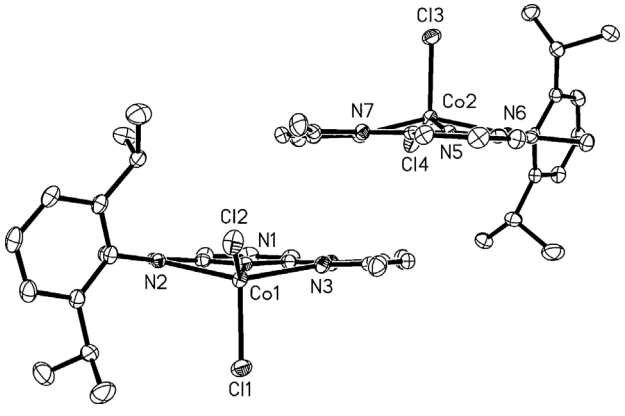

Fig. 3. ORTEP drawing of **5f** with thermal ellipsoids at the 30% probability level. Hydrogen atoms have been omitted for clarity.

2.2.2. Ligand environment effect

The successful characterization of the molecular structures of these Co complexes allowed us to interrogate the influence of the ligand structures on the catalytic performances of the metal center (entries 2 in Tables 1 and 2). Complex **5a** demonstrated the highest total conversion of butadiene of 94%. The resultant polymer possesses predominantly *cis*-1,4 enchainment, with approx. 2.5% of 1,2 and negligible *trans*-1,4 structures. A broad but single GPC peak indicated that multiple sites were involved in the polymerization processes, presumably due to the presence of at least two types of active species derived from the naked $CoCl_4^{2-}$ and the ligated CoL_2^{2+} ions (L: **4a**) by intra- and/or intermolecular ligand redistribution during activation process. Trimethyl-substituted complex **5b** clearly suppressed the monomer conversion, suggesting that bulky groups near the metal center may prevent the access of the monomer to the active site, and lead to the decrease of the polymerization activity. Interestingly, the *cis*-1,4 selectivity witnesses a slightly beneficial effect, an increase from 97.1% to 97.7%, which is an indication that the crowded environment around the metal center is favorable to the *cis*-1,4 selectivity in the current catalytic system. These observations could be rationalized by the fact that the bulky substituents near the active site could reduce the enchainment error during the polymerization. The molecular weight of the polymer obtained was doubled, suggesting that the chain transfer reactions were effectively suppressed in this system. As expected from this trend, the highest selectivity and the lowest conversion were observed for the most crowded (the space around the metal is most crowded) complex **5c** among the **5a–c** triad. While increasing the steric bulk of the ligand could result in an increase in the molecular weight, a slightly smaller molecular weight, calculated to be 169,000, was achieved with **5c**, compared to that obtained from **5b**. This result might be caused by the more severely suppressed chain propagation rate, with a lesser suppressed chain transfer. The substituents on the pyrazole moiety also affected the catalyst performance. The similar trends were observed for the group **5d**–**5f**, with one exception that **5e** gave the highest monomer conversion. Although the exact reason is not yet clear, the synergic effect from methyl groups in the pyrazoyl and iminoaryl moieties may play a role. The highest selectivity of 98.7% was achieved with **5f** at a little expense of conversion. Complex **5g**, possessing the bulkiest environment around the metal center, also showed a high

Table 1
Effect of MAO/Co molar ratio and temperature on butadiene polymerization using **5c**.

Entry	MAO/Co	Temp. (°C)	Time (min)	Yield. (%)	M_n ($\times 10^{-4}$)	PDI	Microstructure (%)		
							Cis-1,4	*Trans*-1,4	1,2
1	400	0	180	42	7.6	1.4	98.7	0.2	1.1
2	400	25	120	72	16.9	1.6	98.0	0.4	1.6
3	400	40	120	66	13.0	2.1	97.6	0.2	2.2
4	400	60	120	41	6.1	2.3	97.2	0.2	2.6
5	400	80	120	11	2.1	2.8	97.2	0.3	2.5
6	100	25	120	44	9.9	2.5	97.3	0.3	2.4
7	200	25	120	62	14.9	2.1	97.8	0.2	2.0
8	600	25	120	83	15.3	1.7	97.8	0.2	2.0
9	1000	25	120	73	11.5	2.0	97.8	0.2	2.0

Polymerization conditions: precursor, 10.0 μmol; butadiene, 30.0 mmol; toluene, 5.0 mL.

Table 2
Butadiene polymerization catalyzed by various cobalt complexes.

Entry	Comp.	Yield (%)	M_n ($\times 10^{-4}$)	PDI	Microstructure (%)		
					Cis-1,4	*Trans*-1,4	1,2
10	**5a**	94	7.9	4.2	97.1	0.4	2.5
11	**5b**	75	18.3	1.3	97.7	0.3	2.0
12	**5d**	72	7.6	1.7	97.6	0.2	2.2
13	**5e**	80	19.1	1.6	98.0	0.2	1.8
14	**5f**	65	11.9	1.9	98.7	0.3	1.0
15	**5g**	61	12.0	1.5	98.0	0.2	1.8
16	**5h**	99	21.5	1.6	97.1	0.4	2.5

Polymerization conditions: precursor, 10.0 μmol; butadiene, 30.0 mmol; MAO (Al), 3.0 mmol; toluene, 5.0 mL; time, 4 h; temperature, 25 °C.

cis-1,4-selectivity of 98.0%. Unfortunately, several attempts in the preparation of cobalt pre-catalysts with **3d**-based imine ligands, which are anticipated for higher selectivity, were not successful, presumably due to the effects of steric congestion. Complex **5h** was thus prepared instead for the examination of polymerization activity. Very interestingly, while a lower *cis*-1,4 selectivity of 97.1% was obtained, quantitative monomer conversion and a high molecular weight were achieved. However, the investigation of ligand effects of complexes derived from analogous ligands, **3a–3c**, could not be conducted due to the inaccessibility of their corresponding cobalt complexes. A plausible active species for these catalysts precursors was shown in Fig. 4

2.2.3. Selectivity regulator

Addition of Lewis bases plays a very important role in the control of activity as well as the stereospecificity in the polymerization of butadiene [29,31,49,70–72]. Among these Co catalysts, the addition of phosphine was examined for altering the regio- and/or stereospecificity of the active species. The incorporation of phosphine as auxiliary ligands to the Co catalyst systems has been demonstrated to afford higher monomer conversions with changes of their selectivity from *cis*-1,4-specific to syndiotactic 1,2-specific [29,31,49,70–72]. As reflected from data in Table 3, both the stereospecificity and monomer conversion can be regulated by the amount and the property of the added phosphine. The addition of 0.25–1.0 equiv. of PPh_3 resulted in the gradually increase of the monomer conversion from 11.3% to 81.1%. More importantly, the 1,2 regio-selectivity was also enhanced from 2.4% to 83.3%, with high syndiotacticity ($rr > 60\%$). ^{13}CNMR analysis has shown that the 1,2 unit was incorporated randomly, rather than producing a blocky microstructure with the 1,4 unit, different from the literature systems [31,33]. This characterization was also supported by the amorphous polymer appearance and the absence of a melting point even at a higher 1,2-enchainmet (entry 20) or syndiotacticity (entry 21). Various 1,2 or 1,4 regio- and stereoselectivities are found, depending on the phosphine structure at 1.0 P/Co molar ratio. Definite trend of catalytic performance in terms of monomer conversion and selectivity with respect to the phosphine structure fails to be concluded, indicating that synergic steric and electronic influences based on the Tolman rule should be considered [73], as neither steric nor electronic factor can clarify the complicated performances. Collectively, PPh_3 proved to be the best choice regarding the monomer conversion and 1,2 regio- and stereoselectivity. A possible role of PPh_3 could be its coordination to the cobalt core, where it served as a protector of active species. A similar effect was also observed in the nickel catalyzed ethylene polymerization or oligomerization systems [74,75]. The widely accepted mechanism for producing the *cis*-1,4-polybutadiene structure proceeds first with the *cis*-1,4 coordination of butadiene to the cobalt center followed by the insertion into the terminal C—Co bond of the cobalt allylic polymer chain. Such a process is favored in the $NNNCoCl_2$ system in absence of additive. By adding phosphine, the monomer insertion mode is shifted, leading to the generation of the 1,2-structure.

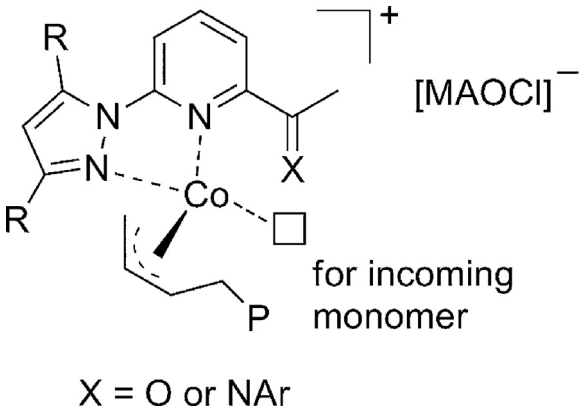

Fig. 4. The proposed active species.

Table 3
Effect of phosphine on polymerization behaviors with **5c**/MAO/phosphine catalyst systems.

Entry	P	P/Co	Yield. (%)	M_n ($\times 10^{-4}$)	PDI	Microstructure (%)			
						1,4	1,2		
							rr (rrrr)	*mr*	*mm*
17	PPh_3	0	11.3	11.1	2.7	97.6	–	–	–
18	PPh_3	0.10	26.3	9.4	2.1	67.5	61.2 (26.4)	36.7	2.1
19	PPh_3	0.25	58.7	8.7	2.1	58.0	61.1 (23.3)	36.2	2.7
20	PPh_3	0.50	59.0	7.9	2.5	55.1	69.8 (17.6)	29.0	1.2
21	PPh_3	0.75	66.6	8.3	2.3	44.0	61.6 (41.3)	37.0	1.4
22	PPh_3	1.0	81.1	8.9	2.4	16.7	64.2 (25.7)	35.6	2.0
23	TFP	1.0	57.1	6.0	2.2	36.6	60.0 (29.9)	31.1	9.0
24	TTMP	1.0	45.2	2.7	2.4	86.3	44.3 (39.0)	55.2	0.5
25	TNP	1.0	44.3	9.6	4.5	87.5	47.0 (22.4)	36.1	16.9
26	TCP	1.0	50.9	7.8	2.6	62.1	51.9 (20.9)	42.6	6.5
27	TMP	1.0	60.7	12.3	2.1	79.1	52.9 (20.8)	42.4	4.7

Polymerization conditions: precursor, 10 μmol; butadiene, 30 mmol; MAO, 3.0 mmol; toluene, 12 mL; time, 1 h; temperature, 25 °C. PPh_3: triphenylphosphine; TFP: tri(2-fluorophenyl) phosphine; TTMP: tri(2,4,6-trimethylphenyl)phosphine; TNP: tri(1-naphthyl)phosphine; TCP: tricyclohexylphosphine; TMP: tri-o-toylphosphine.

3. Conclusion

In summary, a serial of new cobalt complexes carrying unsymmetrical 2-(1-arylimino)-6-(pyrazol-1-yl) pyridine were prepared and fully characterized. The complex **5a** with the smallest-sized ligand was isolated as an ion-pair in the form of $[L_2Co]^{2+}[CoCl_4]^{2-}$, while complex **5f** showed two slightly different geometries in the crystal unit cell. All the complexes converted butadiene selectively to *cis*-1,4-polybutadiene with moderate to high monomer conversion upon activation with MAO. Studies on the ligand effects revealed that bulky groups were crucial for the higher level of *cis*-1,4 selectivity and in general for the higher molecular weight of resulting polymer, accompanied by certain degree of attenuation of the catalytic activity. These observed correlations of catalytic properties and ligand structures may facilitate the development of new catalysts with improved selectivity and activity. The addition of phosphine not only enhanced the monomer conversion but tuned the polymer enchainment from *cis*-1,4 to syndio-1,2 structures, broadening the potential application of this catalytic system.

4. Experimental

4.1. General procedure and materials

$CoCl_2$ and anilines were purchased from Alfa Aesar. 6-Bromo-2-pyridinecarboxylic acid, MAO, pyrazole, 3,5-dimethylpyrazole and butadiene (25 wt% in toluene) were available from Aldrich. Phosphines were purchased either from Strem or Aldrich. Dioxane was dried over CaH_2. Toluene and tetrahydrofuran (THF) were dried with Na/benzophenone and distilled prior to use. ^1H and ^{13}C spectral were recorded on a Bruker AV400 spectrometer at 25 °C with $CDCl_3$ as solvent (400 MHz for ^1H NMR, 100 MHz for ^{13}C NMR). Elemental analyses were conducted by Flash 2000-Thermo Scientific CHNO Analyzer. HRMS was performed on Thermo Scientific™ – LTQ Velos Orbitrap MS using acidified methanol or acetonitrile. IR spectra were performed on JASCO V-670 spectrophotometer. The microstructures of polymers were determined by ^{13}C NMR and ^1H NMR. The number average molecular weights (M_n) and polymer dispersion index (PDI) were measured by VISCOTEK GPC1000 with TDA305 (Triple Detector Array) as detector at 35 °C using THF as eluent (flow rate: 1.0 mL/min) against polystyrene standards.

4.2. X-ray structure determinations

X-ray diffraction data were collected by a Bruker SMART APEX diffractometer with a CCD area detector, using graphite monochromated Mo K radiation (λ = 0.71073 Å). The determination of crystal class and unit cell parameters was carried out by the SMART program package. The raw frame data were processed using SAINT and SADABS to yield the reflection data file. Space groups were determined using XPREP implemented in APEX2. The structures were solved by using SHELXTL-97 (direct method). Refinement was performed by the full-matrix least-squares method on F^2. The hydrogen atoms were added at the calculated positions.

CCDC reference numbers 849,283, 849,284 and 849,285 are for complexes **5a**, **5c** and **5f**, respectively.

4.3. Syntheses and characterizations of ligands and complexes

The representative procedure for the ligand synthesis was modified based on the literature. To a solution of ethyl 6-bromopyridine-2-carboxylate (6.90 g, 30 mmol) in dioxane (150 mL) under argon atmosphere, potassium *tert*-butoxide (3.69 g, 33 mmol) and pyrazole (2.16 g, 31.5 mmol) were added. The resulting mixture was heated at reflux overnight, then cooled to room temperature and quenched by a few drops of water. The solvent was removed and the residue was extracted with ethyl acetate (3× 15 mL) to afford the crude product, which was further purified by column chromatography on silica gel using petroleum ether/ethyl acetate (v/v = 10:1) to give a yellow powder (**2a**, 4.50 g, 70% yield). Compounds **2b** and **2c** were prepared using the same procedure.

2d. Under argon atmosphere, CuI (0.38 g, 2 mmol), proline (0.46 g, 4 mmol) and K_2CO_3 (2.76 g, 20 mmol) were added to a dimethyl sulfoxide (15 mL) solution of 6-bromopyridine-2-carboxylate (4.60 g, 20 mmol) and 3,5-diphenylprazole (4.44 g, 20 mmol). The formed mixture was stirred at 80 °C overnight. Water was added after cooling down to room temperature, and the resulting mixture was extracted with ethyl acetate (3× 20 mL). The organic layers were combined and the solvent was removed to give the crude product, which was purified by column chromatography (3.76 g, 83% yield).

3a. To an ethanol solution of **2a** (4.30 g, 20 mmol), fresh distilled ethyl acetate (7.04 g, 80 mmol) and sodium (2.3 g, 0.1 mol) were added and the reaction mixture was heated at reflux for 5 h. It was then allowed to cool down before 25 mL of concentrated hydrochloric acid was added. The suspension was again heated at reflux with intermittent shaking for 4 h. The mixture was cooled to room temperature, and the organic layer was removed. The aqueous phase was neutralized with sodium carbonate and extracted with ethyl acetate (3× 15 mL). The organic layers were combined and dried over anhydrous sodium carbonate. Compound **3a** was obtained after further purification by column chromatography using petroleum ether/ethyl acetate (v/v = 15:1) (3.24 g, 82%

yield). The same procedure was adopted for the synthesis of compounds **3b–3d**.

4a. To a methanol (25 mL) solution of **3a** (748 mg, 4 mmol), excess aniline (1.82 g, 20 mmol) and three drops of acetic acid were added. The mixture was refluxed overnight, and all volatile was removed under vacuum. The resulting residue was dissolved in methanol (8.0 mL) and recrystallized at −30 °C to give **4a** (833 mg, 80%). The same procedure was adopted for the synthesis of compounds **4b–4f**.

5a. A blue suspension of $CoCl_2$ (63 mg, 2 mmol) in THF was added to a solution of the corresponding ligand (**4a**, 524 mg, 2 mmol) in 10 mL of THF. The reaction mixture was stirred at room temperature overnight, forming a brown precipitate, which was filtered, washed with diethyl ether and hexane. Recrystallization was conducted by slow diffusion of diethyl ether into its saturated dichloromethane solution to give **5a** (511 mg, 87%). The same procedure was adopted for the synthesis of all cobalt complexes.

4.3.1. 6-(Pyrazol-1-yl)-ethylpyridine-2-carboxylate (**2a**)

Obtained as a white solid (4.50 g, 70% yield); ^{1}H NMR (400 MHz, $CDCl_3$, ppm): 8.62 (s, 1H, H_{pyra}), 8.14 (d, 1H, J = 7.8 Hz, H_{pyri}), 8.04 (d, 1H, J = 7.8 Hz, H_{pyri}), 7.95 (t, 1H, J = 7.8 Hz, H_{pyr}), 7.73 (s, 1H, H_{pyra}), 6.48 (s, 1H, H_{pyra}), 4.49 (q, 2H, J = 8.8 Hz, —CH_2CH$_3$), 1.43 (t, 3H, J = 8.8 Hz, —CH_2CH_3). ^{13}C NMR (100 MHz, $CDCl_3$, ppm): 165.11, 154.99, 150.97, 151.52, 143.00, 123.77, 118.89, 113.51, 106.99, 62.00, 13.41.

4.3.2. 6-(3,5-Dimethylpyrazol-1-yl)-ethylpyridine-2-carboxylate (**2b**)

Obtained as a white solid (5.20 g, 85% yield); ^{1}H NMR (400 MHz, $CDCl_3$, ppm): 8.09 (d, 1H, J = 7.6 Hz, H_{pyri}), 7.98–7.95 (m, 2H, H_{pyri}), 6.35 (s, 1H, H_{pyra}), 4.44 (q, 2H, J = 8.8 Hz, —CH_2CH$_3$), 2.75 (s, 3H, —CH_3), 2.25 (s, 3H, —CH_3), 1.41 (t, 3H, J = 8.8 Hz, —CH_2CH_3). ^{13}C NMR (100 MHz, $CDCl_3$, ppm): 165.00, 153.33, 150.40, 146.06, 142.40, 139.13, 121.59, 118.53, 109.57, 61.76, 14.84, 14.31, 13.73.

4.3.3. 6-(3,5-Diisopropylpyrazol-1-yl)-ethylpyridine-2-carboxylate (**2c**)

Obtained as a colorless oil (3.90 g, 54% yield); ^{1}H NMR (400 MHz, $CDCl_3$, ppm): 8.07 (m, 1H, 7.8 Hz, H_{pyri}), 7.98–7.86 (m, 2H, H_{pyri}), 6.01 (s, 1H, H_{pyra}), 4.45 (q, 2H, J = 8.4 Hz, —CH_2CH$_3$), 4.11 (hepta, 1H, J = 8.0 Hz, —$CH(CH_3)_2$), 3.03 (hepta, 1H, J = 8.0 Hz, —$CH(CH_3)_2$), 1.40 (t, 3H, J = 8.4 Hz, —CH_2CH_3), 1.25 (d, 12H, —CH(CH_3)$_2$). ^{13}C NMR (100 MHz, $CDCl_3$, ppm): 164.55, 152.13, 151.42, 147.13, 143.41, 138.53, 120.99, 117.46, 108.31, 60.55, 26.74, 26.21, 23.06, 22.60, 12.89.

4.3.4. 6-(3,5-Diphenylpyrazol-1-yl)-ethylpyridine-2-carboxylate (**2d**)

Obtained as a white solid (3.76 g, 83% yield).^{1}H NMR (400 MHz, $CDCl_3$, ppm): 8.01 (m, 1H, 7.8 Hz, H_{pyri}), 7.87–7.96 (m, 4H, $2H_{Ar}$, $2H_{pyri}$), 7.48–7.36 (m, 8H, H_{Ar}), 6.69 (s, 1H, H_{pyra}), 4.40 (q, 2H, J = 8.4 Hz, —CH_2CH$_3$), 1.44 (t, 3H, J = 8.4 Hz, —CH_2CH_3). ^{13}C NMR (100 MHz, $CDCl_3$, ppm): 165.43, 151.33, 151.10, 145.44, 143.44, 135.52, 133.44, 132.59, 128.99, 128.82, 128.67, 128.21, 128.17, 125.89, 121.44, 117.42, 114.51, 64.22, 11.33.

4.3.5. 6-(Pyrazol-1-yl)-2-acetylpyridine (**3a**)

Obtained as a yellow solid (3.24 g, 82% yield); ^{1}H NMR (400 MHz, $CDCl_3$, ppm): 8.60 (s, 1H, H_{pyra}), 8.16 (d, 1H, J = 7.6 Hz, H_{pyri}), 7.97–7.90 (m, 2H, H_{pyri}), 7.76 (s, 1H, H_{pyra}), 6.50 (s, 1H, H_{pyra}), 2.75 (s, 3H, —CH_3). ^{13}C NMR (100 MHz, $CDCl_3$, ppm): 199.11, 155.01, 151.09, 152.54, 143.04, 123.88, 118.71, 113.46, 106.45, 26.14.

4.3.6. 6-(3,5-Dimethylpyrazol-1-yl)-2-acetylpyridine (**3b**)

Obtained as a yellow solid (4.33 g, 87% yield); ^{1}H NMR (400 MHz, $CDCl_3$, ppm): 8.11 (d, 1H, J = 7.8 Hz, H_{pyri}), 7.86–7.92 (m, 2H, H_{pyri}), 6.03 (s, 1H, H_{pyra}), 2.74 (s, 3H, —CH_3), 2.69 (s, 3H, —C(O)CH_3), 2.30 (s, 3H, —CH_3). ^{13}C NMR (100 MHz, $CDCl_3$, ppm): 199.43, 152.70, 151.20, 150.37, 141.62, 139.22, 118.97, 118.27, 109.73, 26.24, 15.21, 13.65.

4.3.7. 6-(3,5-Diisopropylpyrazol-1-yl)-2-acetylpyridine (**3c**)

Obtained as a yellow oil (4.22 g, 61% yield); ^{1}H NMR (400 MHz, $CDCl_3$, ppm): 8.12 (d, 1H, J = 7.6 Hz, H_{pyri}), 7.87 (m, 2H, H_{pyri}), 6.13 (s, 1H, H_{pyra}), 4.07 (hepta, 1H, J = 6.8 Hz, —$CH(CH_3)_2$), 3.03 (hepta, 1H, J = 6.8 Hz, —$CH(CH_3)_2$), 2.67 (s, 3H, —CH_3), 1.30 (d, 12H, J = 6.8 Hz, —CH(CH_3)$_2$). ^{13}C NMR (100 MHz, $CDCl_3$, ppm): 199.45, 160.49, 153.19, 152.90, 151.31, 139.12, 120.24, 118.46, 102.78, 28.09, 26.74, 26.21, 23.06, 22.60.

4.3.8. 6-(3,5-Diphenylpyrazol-1-yl)-2-acetylpyridine (**3d**)

Obtained as a yellow solid (2.59 g, 55% yield); ^{1}H NMR (400 MHz, $CDCl_3$, ppm): 8.21 (d, 1H, J = 7.8 Hz, H_{pyri}), 7.86–7.97 (m, 4H, $2H_{Ar}$, $2H_{pyri}$), 7.48–7.36 (m, 8H, H_{Ar}), 6.83 (s, 1H, H_{pyra}), 1.89 (s, 3H, —C(O)CH_3). ^{13}C NMR (100 MHz, $CDCl_3$, ppm): 199.41, 152.85, 151.74, 151.12, 145.48, 139.37, 132.61, 132.58, 128.89, 128.78, 128.53, 128.22, 128.10, 126.00, 120.31, 119.16, 107.73, 24.97. Anal. Calcd. For $C_{22}H_{17}N_3O_1$: C, 77.86; H, 5.05; N, 12.38. Found: C, 77.50; H, 5.29; N, 11.99.

4.3.9. 2-[1-(Phenylimino)ethyl]-6-(pyrazol-1-yl)-pyridine (**4a**)

Obtained as a yellow solid (833 mg, 80%); ^{1}H NMR (400 MHz, $CDCl_3$, ppm): 8.61 (s, 1H, H_{pyra}), 8.16 (d, 1H, J = 7.8 Hz, H_{pyri}), 8.07 (d, 1H, J = 7.8 Hz, H_{pyri}), 7.92 (t, 1H, J = 7.8 Hz, H_{pyr}), 7.76 (s, 1H, H_{pyra}), 7.40–7.38 (m, 2H, H_{Ar}), 7.12–7.10 (m, 1H, H_{Ar}), 7.85–7.83 (m, 2H, H_{Ar}), 6.48 (s, 1H, H_{pyra}). ^{13}C NMR (100 MHz, $CDCl_3$, ppm): 166.61, 155.21, 151.13, 150.50, 142.17, 139.21, 129.06, 127.00, 123.77, 119.24, 118.86, 113.31, 107.80, 16.28. IR (KBr, cm^{-1}): 1637 ($\nu_{C=N}$), Anal. Calcd. For $C_{16}H_{14}N_4$: C, 73.26; H, 5.38; N, 21.36. Found: C, 74.01; H, 5.04; N, 21.69.

4.3.10. 2-[1-(2,4,6-Trimethylphenylimino)ethyl]-6-(pyrazol-1-yl)-pyridine (**4b**)

Obtained as a yellow solid (1.34 g, 66%); ^{1}H NMR (400 MHz, $CDCl_3$, ppm): 8.62 (s, 1H, H_{pyra}), 8.24 (d, 1H, J = 8.0 Hz, H_{pyri}), 8.07 (d, 1H, J = 8.0 Hz, H_{pyri}), 7.96 (t, 1H, J = 8.0 Hz, H_{pyri}), 7.76 (s, 1H, H_{pyra}), 6.90 (s, 2H, H_{Ar}), 6.48 (s, 1H, H_{pyra}), 2.29 (s, 3H, =N—CH_3), 2.20 (s, 3H, Ar—CH_3), 2.00 (s, 6H, Ar—CH_3). ^{13}C NMR (100 MHz, $CDCl_3$, ppm): 166.65, 154.95, 151.44, 146.23, 142.14, 139.17, 132.35, 128.59, 126.97, 125.23, 118.67, 113.27, 107.75, 20.75, 17.88, 16.45. IR (KBr, cm^{-1}): 1649 ($\nu_{C=N}$), Anal. Calcd. For $C_{19}H_{20}N_4$: C, 74.97; H, 6.62; N, 18.41. Found: C, 74.63; H, 6.91; N, 18.40.

4.3.11. 2-[1-(2,6-Diisopropylphenylimino)ethyl]-6-(pyrazol-1-yl)-pyridine (**4c**)

Obtained as a yellow solid (870 mg, 69%); ^{1}H NMR (400 MHz, $CDCl_3$, ppm): 8.66 (s, 1H, H_{pyra}), 8.26 (d, 1H, J = 8.0 Hz, H_{pyri}), 8.09 (d, 1H, J = 8.0 Hz, H_{pyri}), 7.98 (t, 1H, J = 8.0 Hz, H_{pyri}), 7.77 (s, 1H, H_{pyra}), 7.20–7.01 (m, 3H, H_{Ar}), 6.51 (s, 1H, H_{pyra}), 2.75 (hepta, 2H, J = 4.8 Hz, —$CH(CH_3)_2$), 2.24 (s, 3H, =N—CH_3), 1.16 (d, 12H, J = 4.8 Hz, —CH(CH_3)$_2$). ^{13}C NMR (100 MHz, $CDCl_3$, ppm): 166.28, 154.79, 150.55, 146.31, 142.28, 139.26, 135.79, 132.49, 127.03, 123.40, 123.06, 122.79, 118.72, 113.30, 107.77, 28.33, 23.22, 22.92, 17.21. IR (KBr, cm^{-1}): 1635 ($\nu_{C=N}$), Anal. Calcd. For $C_{22}H_{26}N_4$: C, 76.27; H, 7.56; N, 16.17. Found: C, 77.01; H, 7.39; N, 16.39.

*4.3.12. 2-[1-(Phenylimino)ethyl]-6-(3,5-dimethylpyrazol-1-yl)-pyridine (**4d**)*

Obtained as a yellow solid (456 mg, 56%); ^{1}H NMR (400 MHz, $CDCl_3$, ppm): 8.10 (d, 1H, J = 8.0 Hz, H_{pyri}), 7.99 (d, 1H, J = 8.0 Hz, H_{pyri}), 7.93 (t, 1H, J = 8.0 Hz, H_{pyr}), 7.39–7.35 (m, 2H, H_{Ar}), 7.12 (t, 1H, J = 6.8 Hz, H_{Ar}), 6.83 (d, 1H, J = 6.8 Hz, H_{Ar}), 6.02 (s, 1H, H_{pyra}), 2.72 (s, 3H, —CH_3), 2.32 (s, 3H, —CH_3), 2.31 (s, 3H, =N—CH_3). ^{13}C NMR (100 MHz, $CDCl_3$, ppm): 164.34, 151.15, 150.02, 141.41, 138.78, 129.03, 123.69, 119.27, 118.03, 116.50, 117.56, 109.29, 16.65, 15.12, 13.69. IR (KBr, cm^{-1}): 1641 ($\nu_{C=N}$), Anal. Calcd. For $C_{18}H_{18}N_4$: C, 74.46; H, 6.25; N, 19.30. Found: C, 74.09; H, 6.14; N, 19.11.

*4.3.13. 2-[1-(2,4,6-Trimethylphenylimino)ethyl]-6-(3,5-dimethylpyrazol-1-yl)-pyridine (**4e**)*

Obtained as a yellow solid (783 mg, 78%); ^{1}H NMR (400 MHz, $CDCl_3$, ppm): 8.28 (d, 1H, J = 7.2 Hz, H_{pyri}), 8.00 (d, 1H, J = 8.0 Hz, H_{pyri}), 7.1 (t, 1H, J = 8.0 Hz, H_{pyr}), 6.89 (s, 2H, H_{Ar}), 6.03 (s, 1H, H_{pyra}), 2.72 (s, 3H, —CH_3), 2.32 (s, 3H, Ar—CH_3), 2.29 (s, 3H, —CH_3), 2.16 (s, 3H, -N = CH_3), 2.01 (s, 6H, Ar—CH_3). ^{13}C NMR (100 MHz, $CDCl_3$, ppm): 166.41, 157.55, 145.92, 144.36, 140.93, 138.75, 132.46, 129.19, 128.61, 125.13, 120.03, 104.11, 20.74, 17.84, 16.60, 12.20. IR (KBr, cm^{-1}): 1644 ($\nu_{C=N}$), Anal. Calcd. For $C_{21}H_{24}N_4$: C, 75.87; H, 7.28; N, 16.85. Found: C, 76.31; H, 7.05; N, 17.11.

*4.3.14. 2-[1-(2,6-Diisopropylphenylimino)ethyl]-6-(3,5-dimethylpyrazol-1-yl)-pyridine (**4f**)*

Obtained as a yellow solid (909 mg, 49%); ^{1}H NMR (400 MHz, $CDCl_3$, ppm): 8.31 (d, 1H, J = 8.0 Hz, H_{pyri}), 8.03 (d, 1H, J = 8.0 Hz, H_{pyri}), 7.92 (t, 1H, J = 8.0 Hz, H_{pyri}), 7.25–7.11 (m, 3H, H_{Ar}), 6.03 (s, 1H, H_{pyra}), 2.76 (hepta, 2H, J = 4.8 Hz, —CH(CH_3)$_2$), 2.74 (s, 3H, —CH_3), 2.32 (s, 3H, —CH_3), 2.20 (s, 3H, =N—CH_3), 1.24 (d, 12H, J = 4.8 Hz, —CH(CH_3)$_2$). ^{13}C NMR (100 MHz, $CDCl_3$, ppm): 152.60, 150.06, 141.48, 138.97, 136.28, 124.11, 123.14, 122.53, 118.42, 116.86, 109.41, 28.39, 23.27, 22.93, 18.34, 17.46, 15.15, 13.66. IR (KBr, cm^{-1}): 1631 ($\nu_{C=N}$), Anal. Calcd. For $C_{24}H_{30}N_4$: C, 76.97; H, 8.07; N, 14.96. Found: C, 77.11; H, 7.92; N, 15.10.

*4.3.15. 2-[1-(2,6-Diisopropylphenylimino)ethyl]-6-(3,5-diisopropylpyrazol-1-yl)-pyridine (**4g**)*

Obtained as a yellow solid (602 mg, 36%); ^{1}H NMR (400 MHz, $CDCl_3$, ppm): 8.33 (d, 1H, J = 8.0 Hz, H_{pyri}), 7.66 (d, 1H, J = 8.0 Hz, H_{pyri}), 7.62 (t, 1H, J = 8.0 Hz, H_{pyri}), 7.17–7.12 (m, 3H, H_{Ar}), 5.89 (s, 1H, H_{pyra}), 2.98 (hepta, 2H, J = 4.8 Hz, —CH(CH_3)$_2$), 2.70 (hepta, 2H, J = 4.8 Hz, —CH(CH_3)$_2$), 2.19 (s, 3H, =N—CH_3), 1.18 (d, 12H, J = 4.8 Hz, —CH(CH_3)$_2$), 1.13 (d, 12H, J = 4.8 Hz, —CH(CH_3)$_2$). ^{13}C NMR (100 MHz, $CDCl_3$, ppm): 165.93, 157.42, 154.96, 146.13, 140.99, 138.78, 135.65, 129.20, 123.81, 123.403, 120.104, 98.42, 28.28, 26.86, 23.21, 22.28, 22.59, 17.296. IR (KBr, cm^{-1}): 1631 ($\nu_{C=N}$), Anal. Calcd. For $C_{28}H_{38}N_4$: C, 78.10; H, 8.89; N, 13.01. Found: C, 77.89; H, 8.71; N, 12.83.

*4.3.16. 2-[1-(Phenylimino)ethyl]-6-(pyrazol-1-yl)-pyridine cobaltdichloride (**5a**)*

Obtained as a brown solid (511 mg, 87%); IR (KBr, cm^{-1}): 1627 ($\nu_{C=N}$), Anal. Calcd. For $C_{16}H_{14}Cl_2CoN_4$: C, 49.00; H, 3.60; N, 14.29. Found: C, 48.71; H, 3.69; N, 14.69.

*4.3.17. 2-[1-(2,4,6-Trimethylphenylimino)ethyl]-6-(pyrazol-1-yl)-pyridine cobaltdichloride (**5b**)*

Obtained as a green solid (433 mg, 92%); IR (KBr, cm^{-1}): 1624 ($\nu_{C=N}$), Anal. Calcd. For $C_{19}H_{20}Cl_2CoN_4$: C, 52.55; H, 4.64; N, 12.90. Found: C, 52.71; H, 4.71; N, 13.09.

*4.3.18. 2-[1-(2,6-diisopropylphenylimino)ethyl]-6-(pyrazol-1-yl)-pyridine cobaltdichloride (**5c**)*

Obtained as a green solid (289 mg, 95%); IR (KBr, cm^{-1}): 1621 ($\nu_{C=N}$), Anal. Calcd. For $C_{22}H_{26}Cl_2CoN_4$: C, 55.48; H, 5.50; N, 11.76. Found: C, 55.70; H, 5.67; N, 11.49.

*4.3.19. 2-[1-(Phenylimino)ethyl]-6-(3,5-dimethylpyrazol-1-yl)-pyridine cobaltdichloride (**5d**)*

Obtained as a green solid (312 mg, 89%); IR (KBr, cm^{-1}): 1622 ($\nu_{C=N}$), Anal. Calcd. For $C_{18}H_{18}Cl_2CoN_4$: C, 51.45; H, 4.32; N, 13.33. Found: C, 51.34; H, 4.56; N, 13.49.

*4.3.20. 2-[1-(2,4,6-Trimethylphenylimino)ethyl]-6-(3,5-dimethylpyrazol-1-yl)-pyridine cobaltdichloride (**5e**)*

Obtained as a green solid (239 mg, 95%); IR (KBr, cm^{-1}): 1629 ($\nu_{C=N}$), Anal. Calcd. For $C_{21}H_{24}Cl_2CoN_4$: C, 54.56; H, 5.23; N, 12.12. Found: C, 54.45; H, 5.45; N, 12.09.

*4.3.21. 2-[1-(2,6-Diisopropylphenylimino)ethyl]-6-(3,5-dimethylpyrazol-1-yl)-pyridine cobaltdichloride (**5f**)*

Obtained as a green solid (322 mg, 93%); IR (KBr, cm^{-1}): 1623 ($\nu_{C=N}$), Anal. Calcd. For $C_{24}H_{30}Cl_2CoN_4$: C, 57.15; H, 6.00; N, 11.11. Found: C, 57.01; H, 5.81; N, 11.09.

*4.3.22. 2-[1-(2,6-Diisopropylphenylimino)ethyl]-6-(3,5-diisopropylpyrazol-1-yl)-pyridine cobaltdichloride (**5g**)*

Obtained as a green solid (387 mg, 83%); IR (KBr, cm^{-1}): 1625 ($\nu_{C=N}$), Anal. Calcd. For $C_{28}H_{38}Cl_2CoN_4$: C, 60.0; H, 6.83; N, 10.00. Found: C, 59.81; H, 6.81; N, 10.23.

*4.3.23. 2-Acetyl-6-(3,5-diisopropylpyrazol-1-yl)-pyridine cobaltdichloride (**5h**)*

Obtained as a blue solid (405 mg, 86%); IR (KBr, cm^{-1}): 1710 ($\nu_{C=O}$), Anal. Calcd. For $C_{22}H_{17}Cl_2CoN_4$: C, 56.55; H, 3.67; N, 11.99. Found: C, 56.41; H, 3.80; N, 12.13.

4.3.24. Representative polymerization procedure

In a glovebox, complex **5c** (4.6 mg, 10 μmol (entry 13, Table 2)) was added into a moisture free ampule bottle. MAO (Al, 3.0 mmol) was then injected, followed by adding a toluene solution of 1,3-butadiene (1.62 g, 30.0 mmol). After a designated time, methanol was injected into the system to quench the reaction. The mixture was poured into 60 ml of methanol containing hydrochloric acid (1.0 mL) to precipitate the polymer. The precipitated polymer was filtered, washed with methanol, and dried under vacuum at 40 °C to a constant weight (1.13 g, 70%).

Acknowledgement

We are grateful for the generous financial support from King Abdullah University of Science and Technology.

Appendix A. Supplementary data

Supplementary data associated with this article can be found, in the online version, at http://dx.doi.org/10.1016/j.apcata.2013.04.026.

References

[1] A. Fischbach, R. Anwander, Adv. Polym. Sci. 204 (2006) 155–281.
[2] L. Friebe, O. Nuyken, W. Obrecht, Adv. Polym. Sci. 204 (2006) 1–154.
[3] L. Porri, G. Ricci, A. Giarrusso, N. Shubin, Z. Lu, Olefin Polym. 749 (2000) 15–30 (Chapter 2).
[4] X. Li, J. Baldannis, M. Nishiura, O. Tardif, Z. Hou, Angew. Chem. Int. Ed. 45 (2006) 8184–8188.
[5] L. Zhang, T. Suzuki, Y. Luo, M. Nishiura, Z. Hou, Angew. Chem. Int. Ed. 46 (2007) 1909–1913.
[6] W. Gao, D. Cui, J. Am. Chem. Soc. 130 (2008) 4984–4991.
[7] K. Endo, Y. Yamanaka, Macromol. Rapid Commun. 20 (1999) 312–314.
[8] L. Porri, G. Ricci, N. Shubin, Macromol. Symp. 128 (1998) 53–61.
[9] R. Cariou, J. Chirinos, V.C. Gibson, G. Jacobsen, A.K. Tomov, M.R.J. Elsegood, Macromolecules 42 (2009) 1443–1444.
[10] L. Porri, M. Aglietto, Makromol. Chem. Macromol. Chem. Phys. 177 (1976) 1465–1476.
[11] C. Ren, G. Li, W. Dong, L. Jiang, X. Zhang, F. Wang, Polymer 48 (2007) 2470–2474.
[12] S. Tobisch, Can. J. Chem-Revue. 87 (2009) 1392–1405.
[13] D. Gong, X. Jia, B. Wang, F. Wang, C. Zhang, X. Zhang, L. Jiang, W. Dong, Inorg. Chim. Acta 373 (2011) 47–53.
[14] K. Endo, Y. Yamanaka, Macromol. Chem. Phys. 202 (2001) 201–206.
[15] D. Wang, S. Li, X. Liu, W. Gao, D. Cui, Organometallics 27 (2008) 6531–6538.
[16] Y. Nakayama, K. Sogo, Z. Cai, H. Yasuda, T. Shiono, Polym. Int. 60 (2011) 692–697.
[17] D.C.D. Nath, T. Shiono, T. Ikeda, Appl. Catal. A: Gen. 238 (2003) 193–199.
[18] F. Bertini, M. Canetti, G. Ricci, Eur. Polym. J. 45 (2009) 923–931.
[19] K. Endo, Y. Uchida, J. Appl. Polym. Sci. 78 (2000) 1621–1627.
[20] J. Lu, Y. Hu, X. Zhang, J. Bi, W. Dong, L. Jiang, B. Huang, J. Appl. Polym. Sci. 100 (2006) 4265–4269.
[21] G. Ricci, D. Morganti, A. Sommazzi, R. Santi, F. Masi, J. Mol. Catal. A: Chem. 204–205 (2003) 287–293.
[22] G. Ricci, A. Boglia, T. Motta, J. Mol. Catal. A: Chem. 267 (2007) 102–107.
[23] G. Ricci, D. Morganti, A. Sommazzi, R. Santi, F. Masi, J. Mol. Catal. A: Chem. 204 (2003) 287–293.
[24] H. Ashitaka, K. Jinda, H. Ueno, J. Polym. Sci. A: Polym. Chem. 21 (1983) 1951–1972.
[25] H. Ashitaka, H. Ishikawa, H. Ueno, A. Nagasaka, J. Polym. Sci. A: Polym. Chem. 21 (1983) 1853–1860.
[26] G. Ricci, C. Bosisio, L. Porri, Macromol. Rapid Commun. 17 (1996) 781–785.
[27] G. Ricci, F. Bertini, A.C. Boccia, L. Zetta, E. Alberti, B. Pirozzi, A. Giarrusso, L. Porri, Macromolecules 40 (2007) 7238–7243.
[28] L. Cao, W. Dong, L. Jiang, X. Zhang, Polymer 48 (2007) 2475–2480.
[29] D. Gong, W. Dong, Y. Hu, J. Bi, X. Zhang, L. Jiang, Polymer 50 (2009) 5980–5986.
[30] G. Ricci, S. Italia, L. Porri, Polym. Commun. 29 (1988) 305–307.
[31] Z. Cai, M. Shinzawa, Y. Nakayama, T. Shiono, Macromolecules 42 (2009) 7642–7643.
[32] L. Porri, A. Giarrusso, G. Ricci, Prog. Polym. Sci. 16 (1991) 405–441.
[33] R. Cariou, J.J. Chirinos, V.C. Gibson, G. Jacobsen, A.K. Tomov, G.J.P. Britovsek, A.J.P. White, Dalton Trans. 39 (2010) 9039–9045.
[34] N.G. Gaylord, T.K. Kwei, H.F. Mark, J. Polym. Sci. 42 (1960) 417–440.
[35] R. Kaulbach, U. Gebauer, C. Mahner, M.D. Lechner, K. Gehrke, Angew. Makromol. Chem. 239 (1996) 107–119.
[36] A. Miyazawa, T. Kase, K. Soga, Macromolecules 33 (2000) 2796–2800.
[37] G. Natta, L. Porri, A. Carbonaro, Makromol. Chem. 77 (1964) 126–138.
[38] P.A.Z. Suarez, F.M. Silva, R.F. Souza, Y.P. Dick, Polym. Bull. 39 (1997) 311–315.
[39] A.R. O'Connor, M. Brookhart, J. Polym. Sci. A: Polym. Chem. 48 (2010) 1901–1912.
[40] S. Tobisch, Macromolecules 36 (2003) 6235–6244.
[41] S. Tobisch, H. Bogel, R. Taube, Organometallics 17 (1998) 1177–1196.
[42] D. Chandran, C.H. Kwak, C.-S. Ha, I. Kim, Catal. Today 131 (2008) 505–512.
[43] S. Jie, P. Ai, B.-G. Li, Dalton Trans. 40 (2011) 10975–10982.
[44] J. Kim, C. Ha, I. Kim, E-Polymers (2006).
[45] D. Gong, B. Wang, H. Cai, X. Zhang, L. Jiang, J. Organomet. Chem. 696 (2011) 1584–1590.
[46] H. Ashitaka, K. Jinda, H. Ueno, J. Polym. Sci. A: Polym. Chem. 21 (1983) 1989–1995.
[47] D.C.D. Nath, T. Shiono, T. Ikeda, Macromol. Chem. Phys. 203 (2002) 1171–1177.
[48] D.C.D. Nath, T. Shiono, T. Ikeda, Macromol. Chem. Phys. 203 (2002) 756–760.
[49] D.C.D. Nath, T. Shiono, T. Ikeda, Macromol. Chem. Phys. 204 (2003) 2017–2022.
[50] D.C.D. Nath, C.M. Fellows, T. Shiono, Macromol. Res. 14 (2006) 338–342.
[51] G. Ricci, A. Forni, A. Boglia, T. Motta, G. Zannoni, M. Canetti, F. Bertini, Macromolecules 38 (2005) 1064–1070.
[52] C. Meermann, K.W. Törnroos, W. Nerdal, R. Anwander, Angew. Chem. Int. Ed. 46 (2007) 6508–6513.
[53] W.M. Dong, K. Endo, T. Masuda, Macromol. Chem. Phys. 204 (2003) 104–110.
[54] G. Ricci, S. Italia, F. Cabassi, L. Porri, Polym. Commun. 28 (1987) 223–226.
[55] G. Kwag, A. Kim, S. Lee, Y. Jang, P. Kim, H. Baik, D. Yoon, H. Jeong, J. Lee, H. Lee, Rubber Chem. Technol. 75 (2002) 907–922.
[56] A. Fischbach, M.G. Klimpel, M. Widenmeyer, E. Herdtweck, W. Scherer, R. Anwander, Angew. Chem. Int. Ed. 43 (2004) 2234–2239.
[57] S. Kaita, Z. Hou, M. Nishiura, Y. Doi, J. Kurazumi, A.C. Horiuchi, Y. Wakatsuki, Macromol. Rapid Commun. 24 (2003) 180–184.
[58] S. Kaita, Z. Hou, Y. Wakatsuki, Macromolecules 32 (1999) 9078–9079.
[59] L. Zhang, M. Nishiura, M. Yuki, Y. Luo, Z. Hou, Angew. Chem. Int. Ed. 47 (2008) 2642–2645.
[60] V.C. Gibson, C. Redshaw, G.A. Solan, Chem. Rev. 107 (2007) 1745–1776.
[61] K. Endo, N. Hatakeyama, J. Polym. Sci. A: Polym. Chem. 39 (2001) 2793–2798.
[62] K. Endo, N. Hatakeyama, Rubber Chem. Technol. 78 (2005) 143–154.
[63] K. Endo, T. Kitagawa, K. Nakatani, J. Polym. Sci. A: Polym. Chem. 44 (2006) 4088–4094.
[64] D. Gong, B. Wang, C. Bai, J. Bi, F. Wang, W. Dong, X. Zhang, L. Jiang, Polymer 50 (2009) 6259–6264.
[65] V. Appukuttan, L. Zhang, C.-S. Ha, I. Kim, Polymer 50 (2009) 1150–1158.
[66] Y. Nakayama, Y. Baba, H. Yasuda, K. Kawakita, N. Ueyama, Macromolecules 36 (2003) 7953–7958.
[67] A.K.T. James, D. Nobbs, R. Cariou, V.C. Gibson, A.J.P. White, G.J.P. Britovsek, Dalton Trans. 41 (2012) 5949–5964.
[68] P. Ai, L. Chen, Y. Tai, S. Jie, B. Li, J. Organomet. Chem. 705 (2012) 51–58.
[69] M. Zhao, Z. Yu, S. Yan, Y. Li, J. Organomet. Chem. 694 (2009) 3068–3075.
[70] D. Gong, W. Dong, J. Hu, X. Zhang, L. Jiang, Polymer 50 (2009) 2826–2829.
[71] Y. Jang, P. Kim, H. Lee, Macromolecules 35 (2002) 1477–1480.
[72] Y. Jang, P. Kim, H. Jeong, H. Lee, J. Mol. Catal. A: Chem. 206 (2003) 29–36.
[73] C.A. Tolman, Chem. Rev. 77 (1977) 313–348.
[74] R. Gao, L. Xiao, X. Hao, W. Sun, F. Wang, Dalton Trans. (2008) 5645–5651.
[75] R. Gao, M. Zhang, T. Liang, F. Wang, W. Sun, Organometallics 27 (2008) 5641–5648.